MOLECULAR AND CELLULAR BIOLOGY, Sept. 1986, p. 3050–3058
0270-7306/86/093050-09$02.00/0

Vol. 6, No. 9

Escherichia coli Aspartate Transcarbamylase: a Novel Marker for Studies of Gene Amplification and Expression in Mammalian Cells

JOSEPH C. RUIZ AND GEOFFREY M. WAHL*

Gene Expression Laboratory, The Salk Institute, San Diego, California 92138

Received 28 February 1986/Accepted 16 May 1986

Eucaryotic expression vectors containing the *Escherichia coli pyrB* gene (*pyrB* encodes the catalytic subunit of aspartate transcarbamylase [ATCase]) and the Tn*5* phosphotransferase gene (G418 resistance module) were transfected into a mutant Chinese hamster ovary cell line posessing a CAD multifunctional protein lacking ATCase activity. G418-resistant transformants were isolated and analyzed for ATCase activity, the ability to complement the CAD ATCase defect, and the ability to resist high concentrations of the ATCase inhibitor *N*-(phosphonacetyl)-L-aspartate (PALA) by amplifying the donated *pyrB* gene sequences. We report that bacterial ATCase is expressed in these lines, that it complements the CAD ATCase defect in *trans*, and that its amplification engenders PALA resistance. In addition, we derived rapid and sensitive assay conditions which enable the determination of bacterial ATCase enzyme activity in the presence of mammalian ATCase.

Gene or sequence amplification is frequently observed when the overproduction of a particular gene product is required for cell function or growth (30). The numerous examples of gene amplifications which span the phylogenetic scale indicate that many regions of the genome are susceptible to molecular remodeling by this process. An understanding of the initial events mediating gene amplification is important for deducing the mechanism(s) of this important contribution to genome plasticity. However, the frequency (e.g., 10^{-5} to 10^{-6}) at which mutants with amplified sequences arise in cultured cell lines is too low to permit molecular analyses of the initial amplification events (30). To overcome the low frequency of amplification, we (34; G. M. Wahl, S. Carroll, P. Gaudray, J. Meinkoth, and J. Ruiz, *in* R. Kucheriapati, ed., *Gene Transfer*, in press; S. Carroll, P. Gaudray, E. Nakkim, M. L. deRose, and G. M. Wahl, unpublished observations) and others (12, 36) have used in vitro gene transfer to identify genomic regions from which amplification of introduced selectable genes can be observed in greater than 1% of the cell population. High-frequency amplification makes it possible to perform molecular studies of the initial events involved in the amplification process (36; Wahl et al., in press).

The optimal characteristics for a gene which is useful for the identification of hyperamplifiable sites by the gene transfer-amplification studies described above include the following. (i) Resistance to the selective agent should arise primarily by amplification of the selectable gene; (ii) the gene should be small; this allows convenient genetic engineering experiments and facilitates rescue into bacteria of the host chromosomal DNA which flanks the integration site and which presumably engenders the hyperamplifiable phenotype; and (iii) it should be possible to discriminate between expression of the introduced gene and the resident cellular gene by a simple procedure to allow the gene transfer experiments to be performed in a variety of cell lines. None of the amplifiable genes currently available (e.g., dihydrofolate reductase, CAD, and adenosine deaminase) fulfill all these criteria. For example, (i) a significant proportion of methotrexate-resistant mutants have alterations other than dihydrofolate reductase gene amplification (14, 27); (ii) the large size (40 kilobase pairs [kbp]) of the CAD gene (the CAD gene encodes a trifunctional protein which contains the first three enzymes of de novo UMP biosynthesis: carbamyl phosphate synthetase, aspartate transcarbamylase [ATCase], and dihydroorotase) complicates the rescue of adjacent host chromosomal regions; and (iii) transfected adenosine deaminase genes can only be differentiated from the endogenous enzyme by isozyme analysis which entails electrophoretic fractionation (21). Therefore, we sought to construct a gene which overcomes these problems.

The ability of procaryotic genes to be suitably engineered for expression in mammalian cells (13, 26, 28) enabled us to design an amplifiable module which fulfills the criteria enumerated above. We placed the 1.3-kbp *pyrB* gene from *Escherichia coli* under the control of either the simian virus (SV40) or the Moloney murine sarcoma virus promoter and placed an SV40 polyadenylation signal at the 3′ end of the gene. This gene encodes the catalytic subunit of ATCase (23) and has an affinity for the ATCase inhibitor *N*-(phosphonacetyl)-L-aspartate (PALA) similar to that of CAD ATCase (4, 6, 15). To assess directly whether the catalytic subunit of bacterial ATCase (hereinafter referred to as bacterial ATCase) could serve as an amplification marker in mammalian cells, we introduced the *E. coli pyrB* gene into Chinese hamster ovary (CHO) cells which have a CAD enzyme with defective ATCase function (0.015 of wild-type ATCase levels [9]). Our results show that the *pyrB* gene is expressed in CHO cells and that selection for PALA resistance results in amplification of the introduced *pyrB* genes. We also derived rapid, sensitive, and quantitative assays for the *pyrB* gene product in the presence of mammalian CAD since the ATCase activities of these two enzymes differ in their pH and temperature optima as well as in molecular weight. Thus, *pyrB* amplification can be assayed by its expression even in the presence of endogenous CAD genes.

Introduction of a bacterial ATCase enzyme into mammalian cells which contain a CAD gene with defective ATCase function also enabled us to study an unresolved and important issue concerning mammalian UMP biosynthesis. In contrast to procaryotes, in which the first three steps of UMP biosynthesis are catalyzed by discrete enzymes, the single polypeptide chain of the CAD protein catalyzes all three of these reactions in mammalian cells (16). It has been

* Corresponding author.

proposed that the eucaryotic multifunctional CAD protein evolved from the combination of three distinct genes to allow coordinate regulation or more efficient substrate utilization by channeling of substrates and products between adjacent catalytic centers (11, 29). By analyzing the growth rates of *pyrB* transformants of mammalian cells containing a functional carbamyl phosphate synthetase and dihydroorotase, we were able to assess whether the bacterial ATCase is catalytically active and is capable of complementing in *trans* the ATCase deficiency of these cells. The implications of our results for the validity of the substrate channeling model are discussed.

MATERIALS AND METHODS

Plasmids. *E. coli* ATCase is encoded by the *pyrB-pyrI* operon (23). An *E. coli* strain (HS1054) containing the *pyrB* locus was a gift of Marc Navre and H. K. Schachman (*pyrB* encodes the catalytic subunit of ATCase and is cloned in pBR322). pSV2*-neo (provided by P. Southern) is a derivative of pSV2-neo (28) in which the *neo* gene including its SV40 promoter, splice, and polyadenylation signals was inserted into the *Bam*HI site of the vector pML. PMSV-1u is a proviral clone of the Moloney murine sarcoma virus inserted at the *Eco*RI site of pBR322 (provided by A. Dusty Miller and Inder Verma).

Construction of expression vectors. To achieve high levels of transcription of the *pyrB* gene in CHO cells, we placed *pyrB* sequences adjacent to either the SV40 early or the Moloney murine sarcoma virus promoter. The SV40 vector used as the parent (pSV2-dhfr [31]) contained the splicing and polyadenylation signals necessary for effective expression. In the second vector, the long terminal repeat (LTR) sequences from the murine sarcoma virus (33) were placed upstream of the *pyrB* gene. The dominant selectable neomycin phosphotransferase gene (*neo*) was then inserted into the *pyrB* recombinant plasmids. The *neo* gene engenders resistance to G418 when present at a single copy per cell (28). The *neo* expression module (which is contained in a 2.6-kilobase *Bam*HI fragment of pSV2*-neo) was inserted into the unique *Bam*HI site of the SV40-*pyrB* construct and into a unique *Bgl*II site downstream from *pyrB* coding sequences in the LTR-*pyrB* construct (see Fig. 1).

The vectors used in these studies are referred to as pSV2-pyrB-neo (pSPN; *neo* in the same transcriptional orientation as *pyrB*), LTR-pyrB-neo (pLPN; *neo* in same transcriptional orientation as *pyrB*), and LTR-pyrB-neo′ (pLPN′; *neo* in the opposite transcriptional orientation as *pyrB*). No eucaryotic polyadenylation signal was present in the *pyrB* transcriptional unit in the pLPN construct, however, in pLPN′, the orientation of the *neo* expression module places the SV40 late polyadenylation signal downstream of *pyrB*.

Cell line, DNA transfection, and PALA selection. D20 is a mutant CHO cell line with a defective CAD protein (provided by David Patterson). The in vitro specific activities of the three enzymatic activities of CAD in D20, represented as a fraction of the CHO-K1 wild-type levels, are 0.53 for carbamyl phosphate synthetase, 0.015 for ATCase, and 0.375 for dihydroorotase (9). This line was maintained in Ham F-12 medium containing 8% fetal calf serum and 60 μM uridine.

Intact circular plasmid DNA was introduced into D20 cells by calcium phosphate coprecipitation (10 μg/10^6 cells in the absence of carrier DNA [7]). Selection for G418-resistant transformants was performed as previously described (28). Isolated G418-resistant transformants for each *pyrB-neo* recombinant plasmid were cloned. The G418-resistant transformants generally contained less than five copies of the transfected plasmid sequences as estimated by Southern blotting (summarized in Table 1).

The plating efficiencies of the G418-resistant transformants were tested in various concentrations of PALA ranging from 0.05 to 10 μM to approximate the ability of *pyrB* to engender PALA resistance. Approximately 1,000 cells were seeded into six-well dishes in F-12–8% fetal calf serum–60 μM uridine, allowed to attach overnight, and then challenged with PALA-containing media. At 6 to 8 days later the plates were fixed (methanol-acetic acid, 9:1 [vol/vol]) and stained with Giesma stain, and the number of colonies was recorded. The plating efficiency data were used to estimate the concentration of PALA which killed 50% of the cells (LD_{50}).

Preparation of cell extracts and enzyme assays. Mammalian cell extracts (~10^7 cells per ml) were prepared by sonication (22) or by freezing and thawing. Bacterial cell extracts were prepared by sonication (10). Protein yields were quantitated with the Bio-Rad assay kit (2).

Bacterial ATCase enzyme activity in cell extracts was screened after electrophoretic fractionation through an acrylamide gel under nondenaturing conditions (M. A. Bothwell, Ph.D. thesis, University of California, Berkeley, 1975). High-molecular-weight standards (Pharmacia Fine Chemicals, Piscataway, N.J.) were included for calibration. The lane containing the molecular weight markers was excised and stained with Coomassie brilliant blue. The remainder of the gel was incubated in a 4°C solution of 1 mM carbamyl phosphate and 20 mM aspartate at pH 7.0 for 10 min. The phosphate produced as a product of the ATCase reaction (carbamyl phosphate + aspartate $\xrightarrow{\text{ATCase}}$ carbamyl aspartate + phosphate) was precipitated in situ with 3 mM lead nitrate. After several rinses in excess cold water, the white lead phosphate precipitate was converted to a more visible brown band by incubation in 5% ammonium sulfide for 10 min. The position of ATCase in the gel is revealed as a brown lead sulfide precipitate, the intensity of which is directly related to the amount of ATCase in the extract. In a native gel system, the catalytic subunit of ATCase migrates as a trimer with a molecular weight of 100,000.

Bacterial ATCase enzyme levels in D20 transformants were quantitated under standard mammalian ATCase assay conditions (22). Briefly, cell extracts were mixed with the ATCase substrates carbamyl phosphate (1.0 mM), L-aspartate (1.6 mM) and L-[U-^{14}C]aspartate (6.5 μCi) in HEPES (*N*-2-hydroxyethylpiperazine-*N*′-2-ethanesulfonic acid) buffer (pH 8.5) and then incubated for 30 min at 37°C. The ATCase specific activity (nanomoles per milligram of protein per hour) was calculated by measuring the conversion of L-[U-^{14}C]aspartate to carbamyl [U-^{14}C]aspartate. To generate pH and temperature profiles of the bacterial and mammalian ATCase activities, HEPES buffer was prepared at pH 8.5, 7.6, and 6.4, and reaction mixtures were incubated for 30 min at 37, 23, 14, or 4°C.

Growth rate determinations. Growth rate analysis of selected lines was performed in Dulbecco modified Eagle medium because we have observed inconsistent growth rates in Ham F-12 medium which was used originally to isolate and propagate D20 (9). The lines were first adapted in Dulbecco modified Eagle medium and nonessential amino acids for several weeks. Generation time estimates were done as follows. On day 1, triplicate 60-mm plates were seeded with 10^4 cells in Dulbecco modified Eagle me-

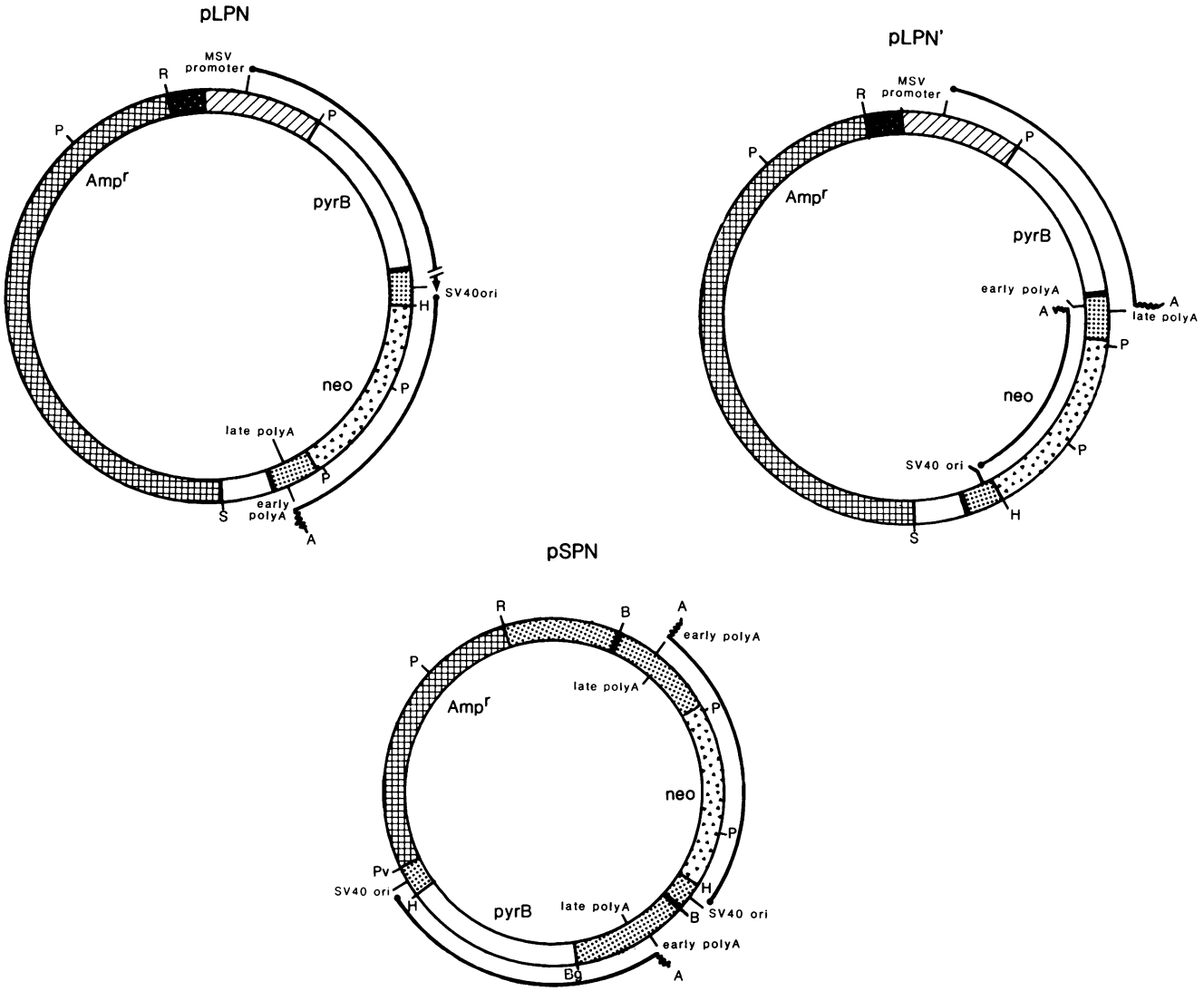

FIG. 1. Structure of *pyrB-neo* recombinant plasmids (see text for details of construction). The *neo* expression module is bounded by thick lines in pLPN, pLPN', and pSPN. Restriction sites: B, *Bam*HI; Bg, *Bgl*II; H, *Hin*dIII; P, *Pst*I; Pv, *Pvu*II; and R, *Eco*RI. ▨, Moloney murine sarcoma virus sequences from LTR to *Pst*I site; ⁞⁞⁞, SV40 sequences including early promoter and early-late polyadenylation signals (32); ▩, *neo* sequences; ▦, pBR sequences; ■, mouse genomic sequences of undetermined location; and □, *pyrB* sequences. ori, Origin.

dium–8% fetal calf serum–nonessential amino acids–60 μM uridine. The next day, the plates were washed and refed medium containing or lacking 60 μM uridine. Cells were fixed onto the plates with 10% trichloroacetic acid on each of the next 5 days and were stored at 4°C until all samples had been collected. The plates were assayed for protein content by a modification of the method of Bramhall et al. (3). The fixed plates were stained with Coomassie brilliant blue G-250 (10 mg/ml in 50% methanol–10% acetic acid) for 15 min. Excess dye was removed quantitatively by three washes with 10% acetic acid. Dye was extracted from the cells with a destaining solution (CH_3OH-H_2O-NH_4OH, 66:34:1). Absorbance of the dye-containing solution was measured at 610 nm against water as a reference. The doubling time was calculated by least-square analysis (days versus $\log_2 A_{610}$).

RESULTS

***pyrB* expression module produces functional ATCase.** Low-copy-number *pyrB* transformants of ATCase-defective (D20) CHO cells were generated by introducing a *pyrB* construct containing *neo* (28) and selecting for G418 resistance (Fig. 1). The G418-resistant transformants generally contained less than five copies of the donated *pyrB-neo* sequences per recipient cell (Table 1).

The active form of the *pyrB* gene product is a trimer with a molecular weight of 100,000 (Bothwell, Ph.D. thesis), whereas the mammalian CAD protein has a native molecular weight of at least 660,000 (5). Therefore it is possible to confirm that bacterial ATCase is synthesized in the G418-resistant *pyrB* transformants by assaying for ATCase activity after electrophoretic fractionation of cell extracts in discontinuous nondenaturing acrylamide gels (Bothwell, Ph.D. thesis). The position of the native ATCase is visualized in the gel by precipitating the phosphate liberated by the ATCase reaction at pH 7.0 and 4°C (carbamyl phosphate + aspartate $\xrightarrow{\text{ATCase}}$ carbamyl aspartate + phosphate; see Materials and Methods). Clones transformed with the *pyrB* plasmid exhibited a band of ATCase activity which comigrated with *pyrB* ATCase activity derived from bacterial extracts

TABLE 1. Characterization of *pyrB-neo* transformants

Cell line	*pyrB* copy no.	ATCase sp act (nmol mg^{-1} h^{-1})	LD_{50} (μM PALA)
CHO-K1	0	45.2	20–30
D20	0	0.5	0.1–0.2
pSPN-2	2–3	7.0[a]	3.5
pSPN-2 S1-3	8–10	95.1[a]	>120
pSPN-5	1–2	1.0[a]	<2.5
pLPN′-2	1–2	15.6[a]	8.0
pLPN′-2 S2-2P	6–8	72.7[a]	ND[b]
pLPN′-3	1–2	1.8[a]	2.5
pLPN-3	1–2	<0.5[a]	ND
pLPN-8	>20	15.2[a]	9.0

[a] Represents bacterial ATCase specific activity: total ATCase specific activity minus endogenous D20 ATCase specific activity.
[b] ND, Not determined.

(Fig. 2). No such band was present in D20 or CHO-K1 cell extracts (Fig. 2, lanes 4 and 5) or in the transformant pLPN-3 (lane 3). The lack of bacterial ATCase expression in pLPN-3 may be due to the absence of a eucaryotic polyadenylation signal downstream of *pyrB* (Fig. 1). The presence of a band of ATCase activity at 100 kilodaltons in the *pyrB-neo* transformants pSPN-2 and pLPN′-2 (lanes 1 and 2) demonstrates that the active form of the *E. coli* ATCase catalytic subunit in animal cells is also a trimer. In addition, the ability to detect ATCase activity in pSPN-2 and pLPN′-2 demonstrates that this assay is sufficiently sensitive to detect the bacterial enzyme in a cell extract prepared from less than 50,000 *pyrB-neo* transformant cells containing one to three copies of the *pyrB* gene (Table 1).

The specific activity of bacterial ATCase in several G418-resistant transformants was determined by the standard assay for mammalian ATCase activity (22). In this assay, the specific activity of ATCase was determined by measuring the conversion of L-[U-^{14}C]aspartate to carbamyl [U-^{14}C]aspartate at pH 8.5 and 37°C (see Materials and Methods). The specific activity of the bacterial enzyme was obtained by subtracting the contribution of D20 ATCase activity from the total ATCase specific activity in extracts of the *pyrB-neo* transformants. All *pyrB-neo* transformants except pLPN-3 exhibited ATCase specific activities exceeding that of D20 (Table 1). The specific activities ranged from 1.0 nmol mg^{-1} h^{-1} for pSPN-5 to 15.6 nmol mg^{-1} h^{-1} for pLPN′-2. The specific activity of pLPN′-2 is approximately 35% of the CHO-K1 ATCase activity level; however, the pyrB and CAD enzymes have different kinetic constants (4, 15, 24), so that it is difficult to make a direct comparison of their specific activities.

The level of *pyrB* expression did not correlate with the number of integrated plasmid molecules. For example, pLPN′-2 and pLPN′-3 have the same copy number, yet the ATCase specific activities differ by 10-fold (Table 1). This difference could be due to the structure of the integrated sequences or the site of integration into the host-cell chromosome or both. The absence of a direct relationship between integrated plasmid copy number and the level of transfected gene expression has been described earlier (8).

The orientation of the G418 resistance module in pLPN′ places the SV40 late polyadenylation signal downstream of *pyrB* (Fig. 1). We confirmed that this site was used for polyadenylation by fractionating total, poly(A)$^-$, and poly(A)$^+$ RNA on a formaldehyde gel (25). The major *pyrB* transcript corresponds to an mRNA which is polyadenylated at a site near the SV40 late polyadenylation signal (data not shown). There is also a minor poly(A)$^+$ mRNA whose length corresponds to polyadenylation at a site in the bacterial sequences downstream from *pyrB*. Interestingly, the sequence AATAAA is present 25 bp downstream from the *pyrB* termination codon (23). The inefficiency of polyadenylation at this site is consistent with the hypothesis that functional polyadenylation signals require additional downstream sequence elements (19, 20; J. Meinkoth, E. Legouy, O. Brison, and G. M. Wahl, Somatic Cell Mol. Genet., in press).

Development of a selective *pyrB* enzyme assay. The bacterial ATCase specific activity for many of the *pyrB-neo* transformants could be determined easily because the endogenous mammalian ATCase activity is negligible in D20. However, for *pyrB* expression to be assayed in cell lines containing wild-type levels of mammalian ATCase, it is necessary to have a rapid and sensitive method for differentiating the expression of *pyrB* from that of the endogenous CAD gene. While the gel assay described above is useful to rapidly screen for cells expressing *pyrB*, it is not straightforward to quantitate the data. The standard mammalian ATCase isotope assay will not differentiate between pyrB and CAD enzyme activities, but rather will provide the sum of the two specific activities. Therefore, conditions were derived which allow the determination of pyrB activity with minimal interference from the mammalian ATCase.

A clue for the derivation of a suitable assay came from the observation that mammalian ATCase activity is not detected in the gel assay. Since proteins of equivalent molecular weight to CAD entered the gels, the two most likely parameters preventing the visualization of mammalian ATCase activity in the gel assay were pH and temperature. We reasoned that one should be able to inhibit mammalian ATCase and leave the bacterial ATCase functional by employing the gel assay conditions for the standard quantitative isotope assay. To test this idea, we determined pH and temperature profiles of CHO and bacterial ATCase. Figure 3A demonstrates that CHO ATCase activity is very sensitive to both pH and temperature. At pH 8.5 and 4°C, the CHO ATCase specific activity is ≤4.0% of what it is at pH 8.5 and 37°C. The same effect is observed for mammalian ATCase

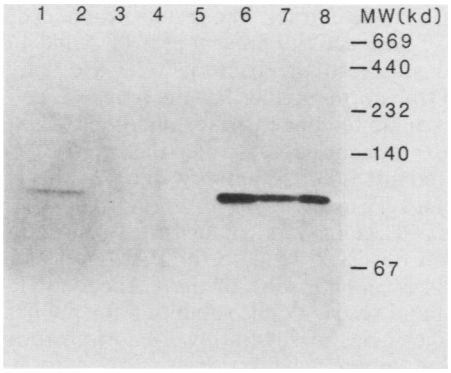

FIG. 2. Nonradioactive assay for bacterial ATCase activity. Cell extract (10 μg except when stated otherwise) was fractionated in a 7.5% acrylamide gel under nondenaturing conditions and assayed in situ for ATCase activity. Lanes: 1, pSPN-2; 2, pLPN′-2; 3, pLPN-3; 4, D20; 5, CHO-K1; 6, bacterial extract from *E. coli* HS1054 (0.2 μg, contains pyrB catalytic subunit) mixed with 10 μg of D20 cell extract; 7, pSPN-2 S1-3 (5 μg), a derivative of pSPN-2 which was selected to resist 60 μM PALA; 8, pLPN′-2 S2-2P (5 μg), a derivative of pLPN′-2 which was selected to resist 100 μM PALA. MW, Molecular weight; kd, kilodaltons.

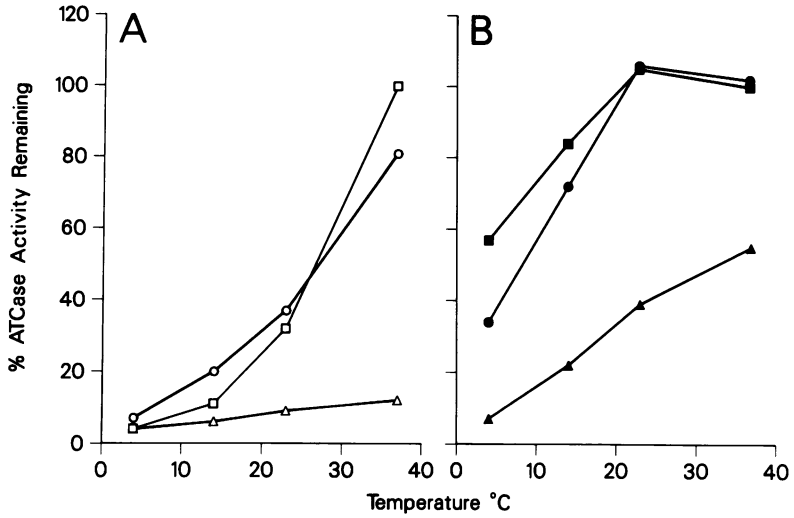

FIG. 3. pH and temperature profiles of mammalian and bacterial ATCase activity. Symbols: □, ■, pH 8.5; ○, ●, pH 7.6; and △, ▲, pH 6.4. (A) CHO ATCase activity. ACTase activity in CHO cell extract (10 μg) was quantitated by an isotope activity assay, and then the specific activities obtained at various conditions were normalized to the specific activity seen at pH 8.5 and 37°C (see text). (B) Bacterial ATCase activity. ATCase activity in pLPN'-2 S2-2P cell extract (5 μg) was quantitated and normalized as above. pLPN'-2 S2-2P is a derivative of pLPN'-2 which was selected to resist 100 μM PALA.

from other cultured cell lines. The ATCase activities at pH 8.5 and 4°C relative to optimal values are: Syrian hamster, ≤2.5%; NIH 3T3 tk$^-$ cells, ≤7%; and mouse L cells, ≤5%. In contrast, pyrB catalytic activity of a *pyrB-neo* transformant is far less sensitive to pH and temperature changes than the mammalian enzyme (Fig. 3B). At pH 8.5 and 4°C, the ATCase specific activity is approximately 60% of that at pH 8.5 and 37°C. These conditions (pH 8.5 and 4°C) produce the maximal difference in ATCase activities between the mammalian and bacterial enzymes. The bacterial ATCase produced in mammalian cells is reproducibly less active at pH 8.5 and 4°C than the enzyme produced by the same gene in *E. coli* (data not shown). The reasons for this difference have not been explored.

We mixed cell extracts prepared from mouse L cells and from a *pyrB-neo* transformant to assess whether the two enzymes could be distinguished from each other when present in a single extract. The results (Table 2) demonstrate that the ATCase activity present at pH 8.5 and 4°C could be attributed solely to the bacterial ATCase activity of the *pyrB-neo* transformant and that the mouse L-cell CAD was effectively inhibited under these conditions (Table no. 3 and 4). This experiment demonstrates that *pyrB* expression can be followed by ATCase activity even in the presence of mammalian ATCase.

***pyrB* as a selectable marker for PALA resistance.** The only mechanism observed to date for PALA resistance in cultured cells is amplification of the CAD gene (1, 17, 34; J. Meinkoth and G. M. Wahl, submitted for publication). The plating efficiencies of several *pyrB-neo* transformants were tested in various concentrations of PALA to approximate the level of PALA resistance engendered by *pyrB*. The transformants pSPN-2, pSPN-5, pLPN'-2, and pLPN'-3 produce bacterial ATCase and exhibit a higher level of PALA resistance than does D20 (i.e., increased LD_{50}; Table 1). In addition, the level of resistance roughly correlates with the enzymatic activity seen in the in vitro assay. The transformants which were tested showed higher plating efficiencies in PALA than did D20, but none approached the plating efficiencies of CHO-K1 (Table 1). This observation is consistent with the fact that these *pyrB-neo* transformants all have lower ATCase specific activities than CHO-K1.

To determine whether amplification of the introduced *pyrB* sequences could engender resistance to high concentrations of PALA, two transformants, pSPN-2 (LD_{50} = 3.5 μM PALA) and pLPN'-2 (LD_{50} = 8 μM PALA), were subjected to increasing concentrations of PALA. pSPN-2 S1-3 is a single-cell clone derivative of pSPN-2 selected to resist 60 μM PALA in one step. Similarly, pLPN'-2 S1-2 is a single-cell clone derived from pLPN'-2 selected to resist 20 μM PALA. A population of cells was subsequently derived from pLPN'-2 S1-2 which was selected to resist 100 μM PALA (referred to as pLPN'-2 S2-2P).

High-molecular-weight DNA was isolated from pSPN-2 S1-3 and pLPN'-2 S2-2P, and the *pyrB* gene copy number was quantitated by the Southern blotting technique to determine whether *pyrB* amplification mediates PALA resistance in the PALA-resistant mutants (Fig. 4A and B). The data in Fig. 4A show that the cloned line pSPN-2 S1-3 has undergone approximately a fourfold amplification of *pyrB-neo* sequences relative to pSPN-2 after a single selection step (lanes 1 and 2). Enzyme analysis confirmed that bacterial ATCase is overproduced in this resistant line (Fig. 2, lane 7). The *Pst*I restriction pattern of the parent pSPN-2 is complex, indicating that various rearrangements occurred upon transfection or integration (compare the pattern of pSPN-2 with

TABLE 2. Quantitation of bacterial ATCase activity in the presence of mammalian ATCase

Cell extract (μg)	ATCase activity (nmol h^{-1} [10^3])		% ATCase activity remaining
	pH 8.5, 37°C	pH 8.5, 4°C	
1. Mouse L (5)	76	2	3
2. pLPN'-2 S2-2P (2.5)	162	96	59
3. Mouse L (5) + pLPN'-2 S2-2P (2.5)	242	96	40
4. Theoretical sum of 1 and 2 (compare with 3)	238	98	41

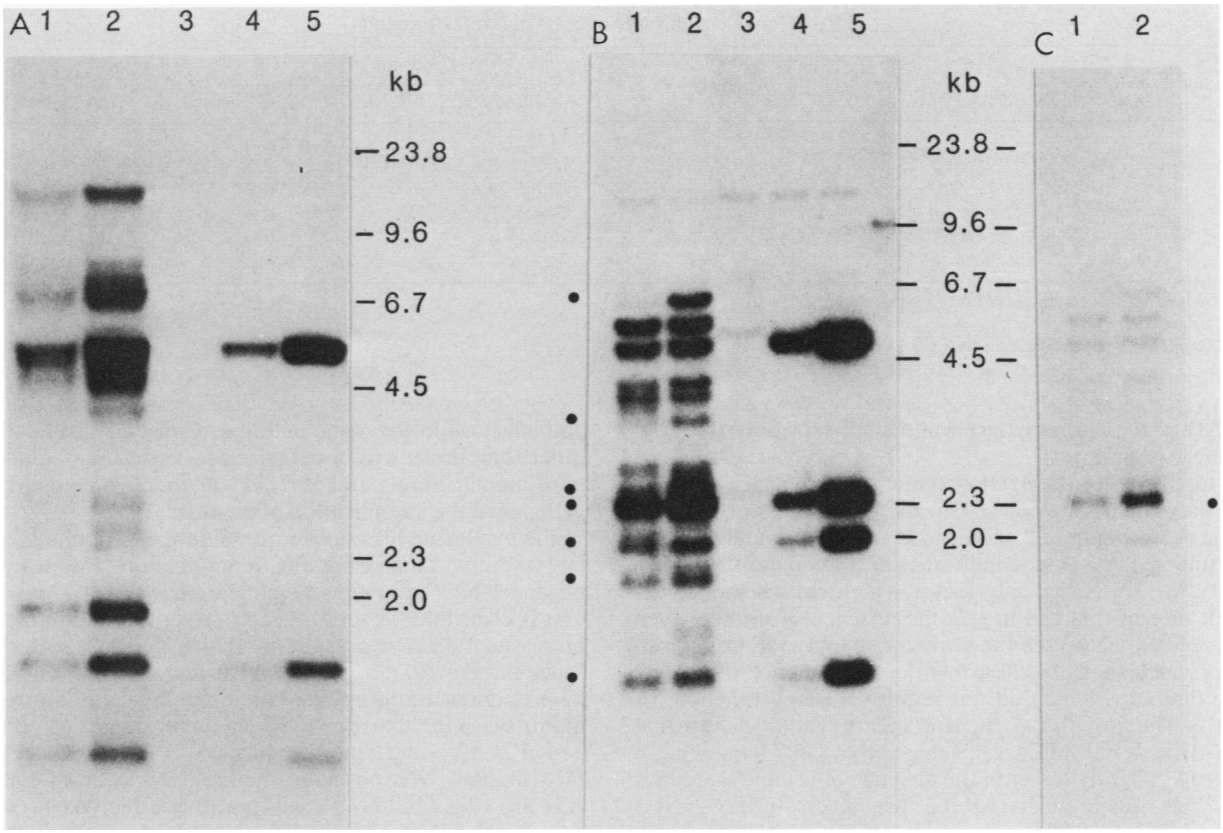

FIG. 4. Restriction analysis of genomic DNA isolated from PALA-resistant derivatives of *pyrB-neo* transformants pSPN-2 and pLPN′-2. (A) Amplified derivative of pSPN-2. *Pst*I-restricted DNA (10 μg) was fractionated in a 0.7% agarose gel, transferred to nitrocellulose, and hybridized to a pSPN nick-translated probe. Lanes: 1, pSPN-2; 2, pSPN-2 S1-3; 3, D20; 4 and 5, a reconstruction experiment containing approximately 1 and 10 copies of *Pst*I-restricted pSPN plasmid, respectively. kb, Kilobases. (B) Amplified derivative of pLPN′-2. *Pst*I-restricted DNA (4 μg) was analyzed as above and hybridized to nick-translated pSPN. Lanes: 1, pLPN′-2; 2, pLPN′-2 S2-2P; 3, D20; 4 and 5, reconstruction experiment containing approximately 1 and 10 copies of *Pst*I-restricted pLPN′ plasmid, respectively. The fragments which are increased in abundance in lane 2 (pLPN′-2 S2-2P) are denoted by the dots. (C) Short exposure of lanes 1 and 2 of panel B. The 2.2-kbp fragment denoted by the dot is the unrearranged *Pst*I fragment seen in pLPN′ plasmid (see lane 4 of panel B) and contains *pyrB* coding sequences.

the *Pst*I restriction pattern of pSPN plasmid in Fig. 4A, lane 5). However, each of the bands present in the parental line is clearly amplified in the PALA-resistant mutant pSPN-2 S1-3. The amplification of each of the bands seen in pSPN-2 indicates that the integrated pSPN vector sequences are only part of a larger DNA unit which has been amplified in pSPN-2 S1-3 (1; Wahl et al., in press). In contrast to this result, the hybridization pattern for pLPN′-2 S2-2P (Fig. 4B) shows that only a subset of *Pst*I restriction fragments homologous to vector sequences and present in pLPN′-2 are amplified (Fig. 4B, lanes 1 and 2). Although the structure of the amplified sequence is difficult to define in this uncloned population of cells, a shorter exposure of this Southern blot shows that the fragment which contains the unrearranged *pyrB* structural gene is amplified approximately fourfold (see labeled fragment in Fig. 4C). Enzyme analysis confirmed that this fourfold increase in the *pyrB* copy number is accompanied by an increase in bacterial ATCase levels (Fig. 2, lane 8). The isolation of PALA-resistant derivatives from two independent *pyrB-neo* transformants demonstrates that the *pyrB* minigene is amplified in PALA-resistant mammalian cells.

Is *pyrB* catalytically active in vivo? The preceding results demonstrate that the overproduction of the 100-kilodalton pyrB trimer mediates PALA resistance in D20 transformants. The presence of a 100-kilodalton trimer in the *pyrB-neo* transformants which comigrates with the authentic bacterial pyrB enzyme in nondenaturing gels suggests that bacterial ATCase is not likely to be associated with the mutant CAD enzyme present in D20 cells. We can envision two mechanisms by which bacterial ATCase could engender PALA resistance. First, the *pyrB* ATCase may not be catalytically active in vivo, but could act merely as a PALA-binding protein which titrates PALA so that the defective ATCase activity of D20 cells can function in the presence of this ATCase inhibitor. Alternatively, the *pyrB* ATCase may not only bind PALA, but may also be active in vivo and contribute to the production of carbamyl aspartate for uridine biosynthesis. If bacterial ATCase can catalyze carbamyl aspartate formation in vivo, then this would indicate that the channelling of substrates in CAD is not an entirely efficient process since it would require the escape of the carbamyl phosphate formed by CAD and the utilization

TABLE 3. Growth rates of *pyrB-neo* transformants

Cell line	ATCase sp act (nmol mg^{-1} h^{-1})	Expt[a]	Growth rate (h)		Ratio of growth rates (−Urd/+Urd)
			+Uridine	−Uridine	
UrdA$^-$[b]	0.3[b]	1	34.7 ± 3.2	No growth	
D20	0.5	1	16.9 ± 0.8	30.7 ± 2.1	1.8
pSPN-2	7.0[c]	1	18.5 ± 0.8	25.0 ± 0.9	1.35
		2	24.4 ± 1.5	29.0 ± 0.9	1.2
pSPN-2 S1-3	95.1[c]	2	26.7 ± 0.6	24.8 ± 0.9	0.93
		3	23.7 ± 1.0	24.2 ± 0.9	1.02

[a] In each experiment a different lot of dialyzed fetal calf serum was used.
[b] Reference 23.
[c] Bacterial ATCase specific activity.

by CAD of the carbamyl aspartate synthesized by the *pyrB* enzyme.

To test whether the *pyrB* enzyme is catalytically active in vivo, the growth rates of D20 in the presence or absence of uridine were compared with those of pSPN-2 and pSPN-2 S1-3 under the same conditions. If the mutant ATCase activity in D20 is the only factor which causes the slower growth rate of this cell line in the absence of uridine, then one would expect to see the growth rate of a *pyrB* transformant approach that of D20 grown in the presence of uridine (i.e., conditions which do not require ATCase function for growth). The growth rate measurements (Table 3) show that pSPN-2 (bacterial ATCase specific activity of 7.0 nmol mg^{-1} h^{-1}) grows slightly faster in the absence of uridine than does D20. With higher bacterial ATCase levels, pSPN-2 S1-3 (specific activity, 95.1 nmol mg^{-1} h^{-1}) grows at the same rate in the presence or absence or uridine. These observations are summarized in Table 3 by the ratio of growth rates in the absence and presence of uridine where a ratio of 1.0 indicates complete complementation. As a control, the growth rate of the CHO uridine auxotroph UrdA$^-$ (22) was measured in uridine-free medium. No growth of UrdA$^-$ occurred in the absence of uridine. The ability of bacterial ATCase to complement the CAD ATCase defect in pSPN-2 S1-3 indicates that bacterial ATCase can catalyze the production of carbamyl aspartate even as a discrete enzyme in mammalian cells and that the defective CAD enzyme in D20 cells can utilize free carbamyl aspartate as a substrate for dihydroorotate synthesis.

DISCUSSION

A bacterial ATCase gene (*pyrB*) under the control of either the SV40 early or Moloney murine sarcoma virus promoter was introduced into mutant CHO cells containing a CAD enzyme with 1.5% of wild-type ATCase activity levels (mutant D20 [9]). Cell extracts of *pyrB* transformants contain the trimeric form of this enzyme which can be distinguished from mammalian ATCase by nonradioactive and radioactive assays. Moreover, in two transformants analyzed, selection for resistance to elevated PALA concentrations gave rise to cells which have amplified *pyrB* sequences. The *E. coli pyrB* gene should, therefore, prove valuable for the study of gene amplification by gene transfer (see Introduction) (Wahl et al., in press) since: (i) PALA resistance is mediated only by ATCase overproduction (i.e., CAD gene amplification [1, 17, 34; this study]); (ii) the small size (1.3 kbp) and favorable restriction map will facilitate molecular analysis of *pyrB*-amplified mutants; and (iii) the ability to rapidly assay bacterial ATCase in the presence of mammalian ATCase will allow one to differentiate between CAD and *pyrB* gene amplification in the same cell line. Consequently, cell lines other than those with a defective ATCase may be used for *pyrB* amplification studies. This will enable a comparison to be made of the amplification of the resident CAD gene to that of the *pyrB* gene introduced into different genomic locations and thereby facilitating the identification of sites which engender high-frequency amplification.

It is clear that bacterial ATCase overproduction mediates increased PALA resistance in D20 Chinese hamster cells. Since the growth rate of the PALA-resistant mutant pSPN-2 S1-3 is the same in uridine-containing and uridine-free medium, we infer that the pyrB enzyme is also catalytically active in vivo and complements the ATCase defect in the D20 mutant. We observed that a low level of bacterial ATCase (e.g., pSPN-2) is not entirely effective in complementing the D20 ATCase defect. This may reflect the fact that the bacterial enzyme has a fourfold-higher K_m for carbamyl phosphate than does mammalian ATCase (K_m [pyrB] = 1.4×10^{-5} M versus K_m [CAD] = 4×10^{-6} M [4, 6, 15]). Furthermore, the bacterial enzyme must draw carbamyl phosphate from the steady-state cellular pool which in D20 is likely to be less than 2×10^{-7} M (4, 9) owing to the depressed carbamyl phosphate synthetase activity of the mutant CAD protein. Therefore, it is not surprising that only higher levels of pyrB enzyme are able to effectively capture carbamyl phosphate for carbamyl aspartate production. The ability of bacterial ATCase to complement the mammalian ATCase defect to various degrees does suggest, at least for the defective CAD protein in D20 cells, that channeling of substrates between the active sites in CAD is not an entirely efficient process. These experiments are consistent with earlier in vitro studies with purified wild-type CAD enzyme which showed that exogenous carbamyl phosphate could enter the uridine biosynthetic pathway through the ATCase reaction (4). In addition, studies in lower eucaryotes demonstrated that contiguous carbamyl phosphate and ATCase enzymes are not required for uridine biosynthesis (11, 18, 35). Our studies provide the first in vivo evidence in mammalian cells that channeling is not essential for de novo UMP biosynthesis. Whether the increased accessibility to unstable substrates afforded by multifunctional proteins has provided subtle growth advantages through evolution or whether such proteins have evolved for coordinate regulation in key biochemical pathways still remain as possibilities to explain the tendencies for the joining of genes encoding enzymes which catalyze successive biochemical reactions in eucaryotic cells (29).

The expression of the *pyrB* constructs introduced into the ATCase-defective D20 cell line can be rapidly and easily quantitated by a sensitive enzyme assay utilizing labeled aspartate. The derivation of assay conditions which enable

the determination of bacterial ATCase activity in the presence of mammalian ATCase may enable *pyrB* to complement the use of the chloramphenicol transferase (*cat*) gene (13) to study gene expression in mammalian cells. The feasibility of such an application will require that the background mammalian ATCase activity (which is ≤5% of the maximal ATCase activity under the differential assay conditions) be significantly lower than the pyrB specific activity. For example, pLPN'-2 has 10 times the level of ATCase activity relative to CHO ATCase at pH 8.5 and 4°C and thus would enable bacterial ATCase to be clearly distinguished from the wild-type mammalian enzyme. On the other hand, other low-copy *pyrB* transformants have appreciably lower levels of expression and would yield only small differences over the endogenous background level. In transient expression experiments in which many functional copies of the gene may be present, the contribution of mammalian ATCase to the total signal could be sufficiently low to enable the use of *pyrB* as an expression marker. Experiments to test this idea are in progress.

ACKNOWLEDGMENTS

We thank H. Schachman and M. Navre for giving us the *pyrB* plasmid and for many helpful discussions; P. Gaudray, J. Meinkoth, N. Proctor, and D. Pauza for critical readings of the manuscript, and M. ter Horst and K. Hyde for their unfathomable patience and expertise in manuscript preparation.

This work was supported in part by Public Health Service grant GM27754 from the National Institutes of Health and by grants from Edward and Lynn Streim and the G. Harold and the Leila Y. Mathers Charitable Foundation. J.R. is a predoctoral student in the Biology Department at the University of California, San Diego, and is supported by National Science Foundation predoctoral minority fellowship.

LITERATURE CITED

1. **Ardeshir, F., E. Giulotto, J. Zieg, O. Brison, W. S. L. Liao, and G. Stark.** 1983. Structure of amplified DNA in different Syrian hamster cell lines resistant to *N*-(phosphonacetyl)-L-aspartate. Mol. Cell. Biol. **3**:2076–2088.
2. **Bradford, M.** 1976. A rapid and sensitive method for the quantitation of microgram quantities of protein utilizing the principle of protein-dye binding. Anal. Biochem. **72**:248–254.
3. **Bramhall, S., N. Noack, M. Wu, and J. R. Loewenberg.** 1969. A simple colorimetric method for determination of protein. Anal. Biochem. **31**:146–148.
4. **Christopherson, R. I., and M. E. Jones.** 1980. The overall synthesis of L-5,6-dihydroorotate by multienzymatic protein *pyr*1-3 from hamster cells. J. Biol. Chem. **255**:11381–11395.
5. **Coleman, P. F., D. P. Suttle, and G. R. Stark.** 1977. Purification from hamster cells of the multifunctional protein that initiates *de novo* synthesis of pyrimidine biosynthesis. J. Biol. Chem. **252**:6379–6385.
6. **Collins, K. D., and G. R. Stark.** 1971. Aspartate transcarbamylase: interaction with the transition state analogue *N*-(phosphonacetyl)-L-aspartate. J. Biol. Chem. **246**:6599–6695.
7. **Corsaro, C. M., and M. L. Pearson.** 1981. Enhancing the efficiency of DNA-mediated gene transfer in mammalian cells. Somatic Cell Genet. **7**:603–616.
8. **Crouse, G. F., R. N. McEwan, and M. L. Pearson.** 1983. Expression and amplification of engineered mouse dihydrofolate reductase minigenes. Mol. Cell. Biol. **3**:257–266.
9. **Davidson, J. N., D. V. Carnright, and D. Patterson.** 1979. Biochemical genetic analysis of pyrimidine biosynthesis in mammalian cells. III. Association of carbamyl phosphate synthetase, aspartate transcarbamylase, and dihydroorotase in mutants of cultured Chinese hamster cells. Somatic Cell Genet. **5**:175–191.
10. **Davidson, J. N., and L. A. Niswander.** 1983. Partial cDNA sequence to a hamster gene corrects defect in *E. coli pyrB* mutant. Proc. Natl. Acad. Sci. USA **80**:6897–6901.
11. **Davis, R. H.** 1967. Channeling in *Neurospora* metabolism, p. 303–322. *In* H. J. Vogel, J. O. Lampen, and V. Bryson (ed.), Organizational biosynthesis. Academic Press, Inc., New York.
12. **Glanville, N.** 1985. Unstable expression and amplification of a transfected oncogene in confluent and subconfluent cells. Mol. Cell. Biol. **5**:1456–1464.
13. **Gorman, C. M., L. F. Moffat, and B. H. Howard.** 1982. Recombinant genomes which express chloramphenicol acetyltransferase in mammalian cells. Mol. Cell. Biol. **2**:1044–1051.
14. **Haber, D., S. M. Beverly, M. L. Kiely, and R. T. Schimke.** 1981. Properties of an altered dihydrofolate reductase encoded by amplified genes in cultured mouse fibroblasts. J. Biol. Chem. **256**:9501–9510.
15. **Hoogenraad, N. J.** 1974. Reaction mechanism of aspartate transcarbamylase from mouse spleen. Arch. Biochem. Biophys. **161**:76–82.
16. **Jones, M. E.** 1980. Pyrimidine nucleotide biosynthesis in animals: genes, enzymes and regulation of UMP biosynthesis. Annu. Rev. Biochem. **49**:253–279.
17. **Kempe, T. D., E. A. Swryrd, M. Bruist, and G. R. Stark.** 1976. Stable mutants of mammalian cells that overproduce the first three enzymes of pyrimidine nucleotide biosynthesis. Cell **9**:541–550.
18. **Lue, P. F., and J. G. Kaplan.** 1970. Metabolic compartmentation at the molecular level: the function of a multienzyme aggregate in the pyrimidine pathway of yeast. Biochim. Biophys. Acta **220**:365–372.
19. **McDevitt, M. A., M. J. Imperiale, H. Ali, and J. R. Nevins.** 1984. Requirement of a downstream sequence for generation of a poly(A) addition site. Cell **37**:993–999.
20. **Nevins, J. R.** 1983. The pathway of eukaryotic mRNA formation. Annu. Rev. Biochem. **52**:441–466.
21. **Orkin, S. H., S. C. Goff, W. N. Kelley, and P. E. Daddona.** 1985. Transient expression of human adenosine deaminase cDNAs: identification of a nonfunctional clone resulting from a single amino acid substitution. Mol. Cell. Biol. **5**:762–767.
22. **Patterson, D., and D. V. Carnright.** 1977. Biochemical genetic analysis of pyrimidine biosynthesis in mammalian cells. I. Isolation of a mutant defective in the early steps of *de novo* pyrimidine biosynthesis. Somatic Cell Genet. **3**:483–495.
23. **Pauza, C. D., M. J. Karels, M. Navre, and H. K. Schachman.** 1982. Genes encoding *Escherichia coli* aspartate transcarbamoylase: the *pyrB-pyrI* operon. Proc. Natl. Acad. Sci. USA **79**:4020–4024.
24. **Porter, R. W., M. O. Modebe, and G. R. Stark.** 1969. Aspartate transcarbamylase: kinetic studies of the catalytic subunit. J. Biol. Chem. **244**:1846–1859.
25. **Rave, N., R. Crkvenjakov, and H. Boedtker.** 1979. Identification of procollagen mRNAs transferred to diazobenzyloxymethyl paper from formaldehyde agarose gels. Nucleic Acids Res. **6**:3559–3567.
26. **Ringold, G., B. Dieckmann, and F. Lee.** 1981. Co-expression and amplification of dihydrofolate reductase cDNA and the *Escherichia coli* XGPRT gene in Chinese hamster ovary cells. J. Mol. Appl. Genet. **1**:165–175.
27. **Sirotnak, F. M., D. M. Moccio, L. E. Kelleher, and L. J. Goutas.** 1981. Relative frequency and kinetic properties of transport-defective phenotypes among methotrexate-resistant L1210 clonal cell lines derived *in vivo*. Cancer Res. **41**:4447–4452.
28. **Southern, P. J., and P. Berg.** 1982. Transformation of mammalian cells to antibiotic resistance with a bacterial gene under control of the SV40 early region promoter. J. Mol. Appl. Genet. **1**:327–341.
29. **Stark, G. R.** 1977. Multifunctional proteins: one gene—more than one enzyme. Trends Biochem. Sci. **2**:64–66.
30. **Stark, G. R., and G. M. Wahl.** 1984. Gene amplification. Annu. Rev. Biochem. **54**:447–491.
31. **Subramani, S., R. Mulligan, and P. Berg.** 1981. Expression of the mouse dihydrofolate reductase complementary deoxyribonucleic acid in simian virus 40 vectors. Mol. Cell. Biol. **1**:854–864.

32. **Subramani, S., and P. J. Southern.** 1983. Analysis of gene expression using simian virus 40 vectors. Anal. Biochem. **135:**1–15.
33. **Van Beveren, C., F. van Straaten, J. A. Galleshaw, and I. M. Verma.** 1981. Nucleotide sequence of the genome of a murine sarcoma virus. Cell **27:**97–108.
34. **Wahl, G. M., B. R. de Saint Vincent, and M. L. DeRose.** 1984. Effect of chromosomal position on amplification of transfected genes in animal cells. Nature (London) **307:**516–520.
35. **Williams, L. G., S. A. Bernhardt, and R. H. Davis.** 1971. Evidence for two discrete carbamyl phosphate pools in *Neurospora*. J. Biol. Chem. **246:**973–978.
36. **Wilson, D. J., S. D. Hanes, M. H. Pichler, and D. K. Biswas.** 1983. 5-Bromodeoxyuridine-induced amplification of prolactin gene is an extrachromosomal event. Biochemistry **22:**6077–6084.